

# Experimental Verification of Target Shadow Parameter Estimation in GPS FSR

Chr. Kabakchiev  
Sofia University  
Sofia, Bulgaria  
ckabakchievr@fmi.uni-sofia.bg

I. Garvanov  
ULSIT  
Sofia, Bulgaria  
i.garvanov@unubit.bg

V. Behar  
IICT-BAS  
Sofia, Bulgaria  
behar@bas.bg

D. Kabakchieva  
UNWE  
Sofia, Bulgaria  
dkabakchieva@unwe.bg

K. Kabakchiev  
University of Birmingham,  
Birmingham, UK  
kalin.kabakchiev@gmail.com

H. Rohling  
TU Hamburg-Harburg  
Hamburg, Germany  
rohlingr@tu-harburg.de

K. Kulpa  
TU Warsaw  
Poland  
kulpa@ise.pw.edu.pl

A. Yarovoy  
TU Delft  
The Netherland  
a.yarovoy@ircr.tudelft.nl

*Abstract*— In this paper we analyze the power budget and calculate signal to noise ratio (SNR) and radar cross section (RCS) for different ground targets using a forward scattering radar (FSR) system, which consists of a transmitter mounted on a satellite of GPS and a receiver located on the Earth's surface. The FSR is a specific bistatic radar system where the bistatic angle is near  $180^\circ$ , and the target is located near the transmitter-receiver baseline. Theoretical and numerical calculations of SNR and RCS are presented for different ground targets when the GPS L1 signal is transmitted by satellites. The SNR and RCS are also estimated by using real records of the GPS signal shadows from different targets. The obtained numerical and experimental results are analyzed and discussed.

**Keywords**— FSR, GPS, parameter estimation

## I. INTRODUCTION

The forward scattering radar is a special type of bistatic radar when the bistatic angle is near  $180^\circ$ , and the target is located near the transmitter-receiver baseline [1, 2]. In FSR, the Babinet's principle is exploited to form the forward scatter signature of a target [3-6]. According to this principle, the drastic enhancement in scattering is created due to the forward scattering phenomenon. At forward scattering, the presence of a target blocks the signal wave front from the transmitter. According to the EM field theory given in [1], when there is an absolutely black body that is placed in the path of wave propagation and the dimensions of this body are large compared with the wavelength, then a scattered field exists behind the body (a 'shadow' field). This target shadow is an electromagnetic field, which is scattered by the target. When bistatic angle approaches  $180^\circ$ , the level of the signal reflected from the target is maximal, and the target can be characterized by a forward scattering cross-section that depends on the target shadow silhouette area [7, 8].

In this paper we calculate and estimate SNR and RCS for different ground targets using FSR, consisting of a satellite-based transmitter and a receiver located on the Earth's surface.

## II. SIGNAL PROCESSING

The general block-scheme for target radio shadow detection using a Software-Defined GPS receiver [9] is shown in Fig.1.

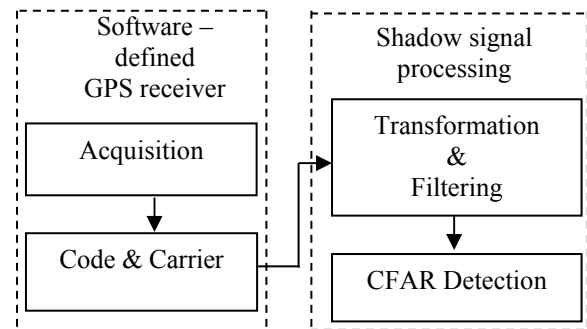


Fig. 1. General block-scheme of signal processing

According to Fig.1, in the software-defined GPS receiver, the inphase quadrature component of the signal at the output of the Code&Carrier block ( $I_p$ ) is obtained in result of execution of a set of program files for acquisition and tracking, presented in [9]. The signal  $I_p$  is further transformed as follows:

$$y = [(x - \max(x))]^2, \text{ where } x = \text{abs}(I_p) \quad (1)$$

This transformation is necessary for further signal detection by CFAR detector. The SNR of the signal  $y$  is further improved by filtering using the Moving Averaging Filter. According to the CFAR detection approach based on the criterion of Neyman – Pearson, the following algorithm can be used for testing a simple hypothesis  $H_1$  (target is present) against a simple alternative  $H_0$  (target is absent):

$$H_1 : \text{if } \max \{y_f(n)\} \geq T_{fa} \cdot \sum_{l=1}^L y_f'(l) \quad (2)$$

$$H_0 : \text{otherwise}$$

In the decision rule (2),  $y_f^l(l)$  are the values of the filtered signal within the reference window of size  $L$  needed for power noise estimation. The detection constant  $T_{fa}$  is determined in accordance with the probability of false alarm  $P_{fa}$ , which should be maintained by the detection algorithm. In case of mean zero Gaussian noise, the detection constant is:

$$T_{fa} = P_{fa}^{-1/L} - 1 \quad (3)$$

### III. POWER BUDGET OF GPS FSR

In case of passive radar that uses signals from GPS satellites, the basic radar equation can be written as:

$$SNR_{det} = \frac{P_t G_r \sigma_0}{4\pi R_{ig}^2 N_r} G_{sp} G_{incoh} \quad (4)$$

In (4),  $SNR_{det}$  is the SNR at the detector input,  $\sigma_0$  is the target radar cross section (RCS),  $R_{ig}$  is the distance to the target,  $P_t$  is the nominal input signal strength of the L1 C/A code is ( $P_t = -160$  dBW),  $N_r$  is the thermal noise at room temperature of 290 K ( $N_r = -141$  dBW),  $G_{sp}$  is the coherent processing gain at the output of the acquisition block and  $G_{incoh}$  is the incoherent processing gain at the output of the Code&Carrier block. The null-to-null bandwidth of the main lobe of the spectrum of L1 C/A code  $\Delta f = 2.046$  MHz and the C/A code length is  $T_s = 1$  ms. Therefore the coherent processing gain is  $G_{sp} = 10 \log_{10}(\Delta f \cdot T_s) = 33.1$  dB. The incoherent processing gain can be computed as  $G_{incoh} = 10 \log_{10}(N)$ , where  $N$  is the number of incoherently integrated samples at the output of the Code&Carrier block. In our calculations we assume  $N = 200$ , therefore  $G_{incoh} = 23.01$  dB. In our experiments, the omnidirectional antenna is used to receive signals from satellites, so the receiver antenna gain  $G_r$  in (4) is assumed to be  $G_r = 0$  dB. From (4) follows that the target RCS can be expressed as a function of SNR at the detector input as follows:

$$\sigma_0 = \frac{4\pi SNR_{det} R_{ig}^2 N_r}{P_t G_r G_{sp} G_{incoh}} \quad (5)$$

The maximal target detection range can be also calculated as a function of SNR as follows:

$$R_{max} = \sqrt{\frac{P_t G_r \sigma_0}{4\pi N_r SNR_{det, min}} G_{sp} G_{incoh}} \quad (6)$$

In case of the Forward Scattering (FS) effect, when the target is located almost on the line "satellite-receiver" or when the bistatic angle is very close to  $180^\circ \pm 2^\circ$ , the target RCS strongly increases (Fig. 2) [10] and depends on the target silhouette area and can be calculated as:

$$\sigma_{FSR} = 4\pi(hl / \lambda)^2 \quad (7)$$

Where  $h$  and  $l$  are respectively the height and the length of the target and  $\lambda$  is the wavelength of the carrier signal emitted by satellites ( $\lambda = 0.19$  m - for the C/A code). Therefore, in case of FSR the target RCS  $\sigma_0$  in equations (4) and (5) must be replaced by  $\sigma_{FSR}$  calculated by (7) [10].

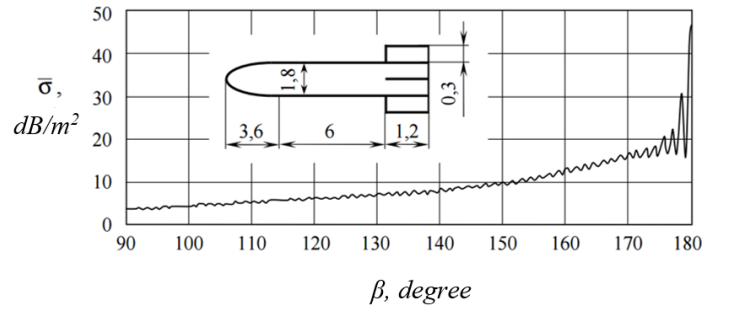


Fig. 2. Target RCS

The results of numerical calculations of  $\sigma_0$  and  $\sigma_{FSR}$  of different ground targets obtained by (5) and (7) are shown in Table 1.

TABLE I. RADAR CROSS SECTION

Target	$\sigma_0$		$\sigma_{FSR}$	
	m <sup>2</sup>	dB	m <sup>2</sup>	dB
pedestrian	1	0	348	25.42
car	3	4.77	5560	37.46
van	6	7.78	34810	45.42
bus	10	10	217560	53.37

As shown, in case of the Forward Scattering (FS) effect, the target RCS, i.e.  $\sigma_{FSR}$ , increases by 20÷40 dB compared to  $\sigma_0$ .

### IV. EXPERIMENTAL PARAMETER ESTIMATION OF GPS SHADOW

In this experimental study, the GPS L1-based recording system consists of two types of GPS receivers. The first GPS receiver (Antaris AEK-4R) is used to determine the location of the satellites while the other software GPS receiver (GNSS\_SDR) is used to record and store GPS signals from different targets (Fig. 3).



Fig. 3. Experimental equipment

In order to record shadows from vehicles should be selected only such satellites that are low located over the horizon. In the experiment scenario, this condition for the occurrence of FS-GPS effect was fulfilled. The experiment scenario includes the stationary-based GPS receiver system that receives and records FS shadows created by vehicles moving on the road (Fig. 4). The GPS receiver is positioned from the one side of the road and 1 m above the ground (Fig. 4). For recording are selected such visible satellites, which are located at low elevation angles and form a baseline (between satellite and receiver), which is a

perpendicular to the road, in order to form the FS effect and create the radio shadow. During the experiment the satellite signals are recorded when different targets (pedestrian, cars, vans, buses etc.) passing on the road. As shown in figure 4, the satellite number 3 is located at the lowest elevation over the horizon, and therefore the bistatic angle should be close to 180 degrees. In that case the targets cross the baseline "satellite – receiver" at the angle of about 90 degrees. This experiment clearly demonstrates the principle of FSR using the GPS receiver.

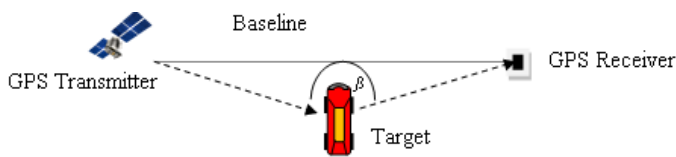
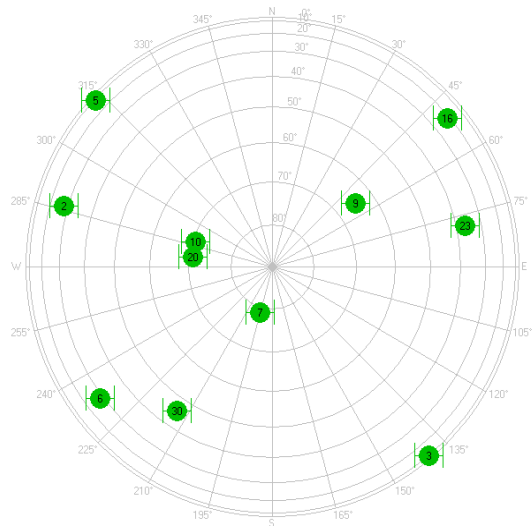


Fig. 4. GPS-FS scenario

As shown in figure 4, the signal received from the satellite number 3 is further processed in the Acquisition and Code&Carrier blocks of the software-defined GPS receiver. Specific programs in Matlab that implement the acquisition and Code&Carrier tracking functions are used in order to extract the navigation message received from the satellite. The extracted navigation message from the satellite is next filtered by the MAFJW with the window length of 200 samples. The output signal of the MAFJW is shown in Fig. 5. It can be seen that the parameters of radio shadows (depth and length of signal fallings) are different for different vehicles (bus or cars)

and, therefore they can be used to classify different moving targets. In order to estimate SNR and the RCS of targets, the target shadow in Fig. 5 is transformed according to (1). The transformed signal is shown in figure 6.

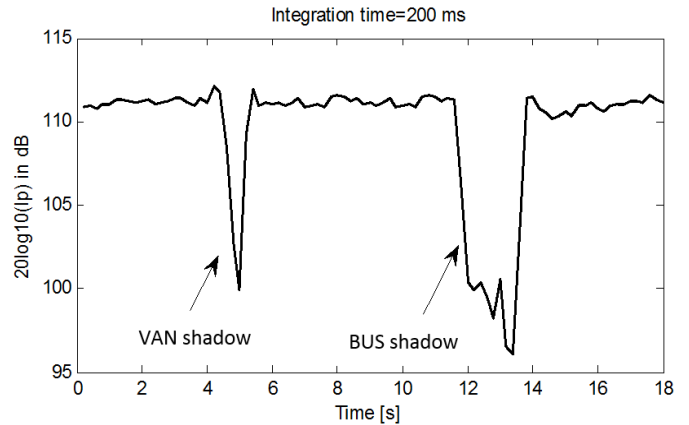


Fig. 5. Radio shadows from a van and a bus (integrating signal)

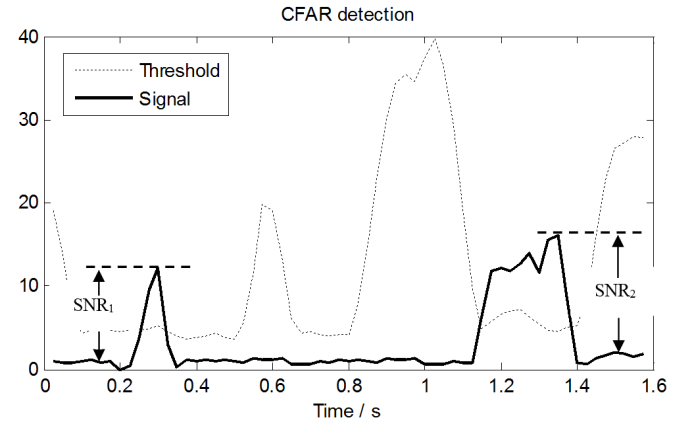


Fig. 6. Invert signal and CFAR threshold

Using a set of recordings of radio signals containing different shadows of ground targets is done the averaging of their SNR for two values of the distance between the receiver and the target (3 to 6 meters). The estimated values of SNR of different vehicles are summarized in Table 2.

TABLE II. EXPERIMENTAL RESULTS FOR SNR

Target distance $R_{tg}$	Car $\sigma = 3 \text{ m}^2$	Van $\sigma = 6 \text{ m}^2$	Bus $\sigma = 10 \text{ m}^2$
	SNR [dB]		
3 m	6	12	15
6 m	2	6	9

The aim of this study is to verify whether the received experimental results are due to bistatic or FS radar system configuration. The numerical calculations of SNR as a function of "target-receiver" distance are obtained using the RCS of targets under study (car, van, bus)  $\sigma_0$  and the basic radar equation (4) for a bistatic radar system. For comparison the numerical calculations of SNR, theoretical values and

experimental estimates, obtained for a bistatic radar system are shown in Fig. 7.

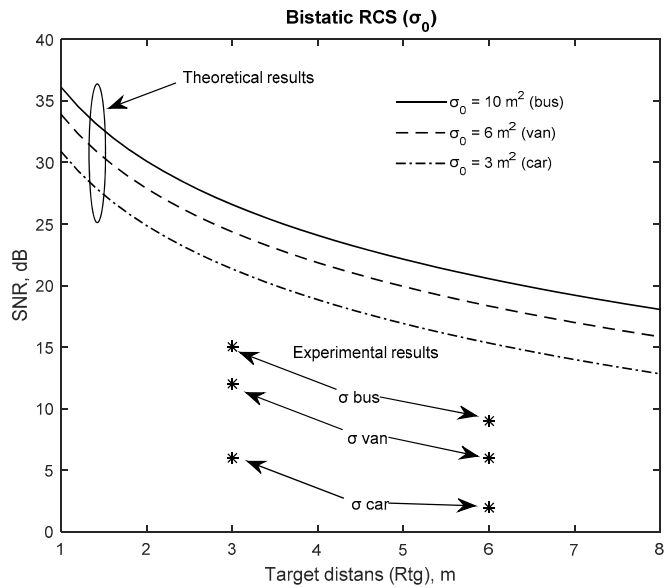


Fig. 7. Numerical calculations of SNR

The theoretical values of SNR calculated for a FSR radar system are shown in Fig. 8 together with the experimental estimates of SNR. In that case the RCS values are higher than those in case of bistatic radar.

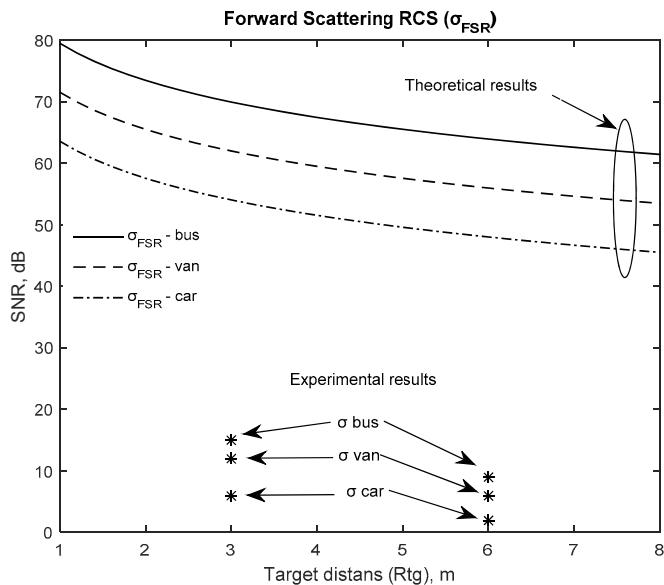


Fig. 8. The calculated values of RCS

From Fig. 7 and Fig. 8 follows that the obtained experimental results are close to the theoretical results obtained for a bistatic radar system.

The analysis of the obtained results shows that the experimental values of the received SNR and RCS are less than their theoretical values. In that case, naturally arises the

following question “What is the reason for the appearance of such a difference between theoretical and experimental results?”

The first reason is that despite the fact that the projection of the baseline “satellite-receiver” is crossed by the target at an angle close to  $90^\circ$ , the real bistatic angle is less than  $180^\circ$ , because the receiver and the satellite are located at different heights from the ground ( Fig. 9).

It can be seen that the conditions for the appearance of the forward scatter effect are fulfilled only partly. The bistatic angle is out of diapason  $180^\circ \pm 2^\circ$ , which is the condition for the appearance of the FS effect.

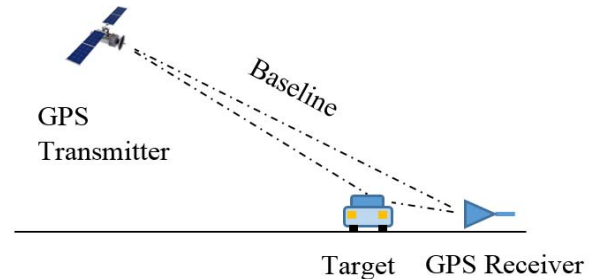


Fig. 9. GPS-FS scenario

The second reason is that during the experiment the energy of the signal received by the GPS receiver is significantly smaller than that which we accepted in theory. The signal transmitted by satellite at low elevation angles spread like GSM signal, overcoming various obstacles located on the surface of the earth. These are the hills, low buildings in the suburbs, high administrative and residential buildings in the town. The signal transmitted by satellite upon its propagation is subject to two main types of attenuation: long-term attenuation - due to propagation losses, losses from shading and short-term attenuation - due to multipath propagation, Doppler signal expansion.

However, regardless of the propagation loss in SNR the obtained results for RCS show that the conditions for the appearance of the FS effect are not fulfilled during the experiment.

#### CONCLUSIONS

The obtained results demonstrate that during the experiment, there was no forward scatter effect. This is due to the fact that the restrictions imposed on the bistatic angle to be 2-3 degrees near 180 degrees are difficult for implementation and require special means to control this angle. During our experiment, it was no possibility to control this bistatic angle between the directions "satellite - receiver" and "target-receiver". In practice this angle could be controlled using a set of narrow antennas of the receiver. In our case we obtained the estimates of target backscattering RCS, i.e.  $\sigma_0$  calculated by (5).

#### ACKNOWLEDGMENT

This work is partly supported by the project DFNI-T 02/3/2014.

## REFERENCES

- [1] Chernyak, V., "Fundamentals of Multisite Radar Systems", Gordon and Breach Science Publishers, 1998, pp. 41.
- [2] Cherniakov M., R.S.A.R. Abdullah, P. Jancovic, M. Salous and V. Chapursky "Automatic ground target classification using forward scattering radar", IEE Proc.- Radar Sonar Navig., Vol. 153, No. 5, October 2006, pp. 427 – 437.
- [3] Kabakchiev C., I. Garvanov, V. Behar, H. Rohling, "The Experimental Study of Possibility for Radar Target Detection in FSR Using L1-Based Non-Cooperative Transmitter", Proc. of IRS'13, Dresden, Germany, 2013, pp.625-630.
- [4] Kabakchiev C., I. Garvanov, V. Behar, D. Kabakchieva, K. Kabakchiev, H. Rohling, K. Kulpa, A. Yarovoy, "Signal Processing of GPS Radio Shadows Formed by Moving Targets", Proc. of SPS'2015, Debe, Poland, 2015.
- [5] Kabakchiev C., I. Garvanov, V. Behar, D. Kabakchieva, K. Kabakchiev, H. Rohling, K. Kulpa, A. Yarovoy, "Detection and Classification of Objects from Their Radio Shadows of GPS Signals", Proc. of IRS'2015, Dresden, Germany, 2015, pp. 906-911.
- [6] Kabakchiev C., V. Behar, I. Garvanov, D. Kabakchieva, L. Daniel, K. Kabakchiev, M. Gashinova, M. Cherniakov, "Experimental verification of maritime target parameter evaluation in FSR", IET Radar, Sonar & Navigation, Volume 9, Issue 4, 1 April 2015, Pages 355-363
- [7] Glennon E., A. Dempster, and C. Rizos, "Feasibility of air target detection using GPS as a bistatic radar", Journal of Global Positioning Systems, 2006, vol. 5, no. 1-2, pp. 119-126.
- [8] Behar V., C. Kabakchiev, H. Rohling, "Air Target Detection Using Navigation Receivers Based on GPS L5 Signals", Proc. of ION GNSS' 2011, Portland OR, 2011, pp. 333-337.
- [9] Borre K., D. Akos, N. Bertelsen, P. Rinder, S. Jensen, "A Software-Defined GPS and Galileo Receiver: Single-Frequency Approach", Birkhäuser, Boston, MA, 2006
- [10] Ковалев Федор Николаевич, "Методы, модели и алгоритмы просветной радиолокации", Нижегородский государственный технический университет им. Р. Е. Алексеева, Диссертация на соискание ученой степени доктора технических наук, Нижний Новгород – 2015, с. 378